

# Dynamics and Scaling of Internally Cooled Convection

Lokahith Agasthya<sup>a</sup>, Caroline Jane Muller<sup>a</sup>

<sup>a</sup>*Institute of Science and Technology Austria, Am Campus  
1, Klosterneuburg, 3400, Austria*

---

## Abstract

Our goal is to investigate fundamental properties of the system of internally cooled convection. The system consists of an upward thermal flux at the lower boundary and a constant cooling term in the bulk. This simple model represents idealised dry convection in the atmospheric boundary layer, where the bulk cooling mimics the radiative cooling to space notably through longwave radiation. We introduce a lapse-rate dependent dimensionless Rayleigh-number that determines the behaviour of the system and the critical Rayleigh-number for transition to convection is obtained numerically. The dynamic behaviour of the fluid system is described and we also infer the scaling of various important measured quantities such as the total vertical convective heat flux and the upward mass flux. We conclude with a short discussion on the relevance to atmospheric convection and the scope for further investigations of atmospheric convection using similar simplified approaches.

---

## 1. Introduction

The study of thermal, convective systems has a long history going back to the late 19th century, with the recorded observations of James Thomson ([1]) and the systematic experiments performed by Henri Bénard [2] setting the stage for further investigation into the effects of heating a fluid. Lord Rayleigh was the first to analytically describe the convective instability resulting from heating a fluid from below [3] using a model system that was named Rayleigh-Bénard (R-B) convection and one that has become the bedrock of studies on the behaviour of thermal fluids and phenomena such as pattern formation, transition to chaos etc.

One of the primary motivations to study R-B convection and other similar model fluid systems is to understand and characterise the behaviour of

the earth's atmosphere. The atmospheric circulation of the earth is driven primarily by the heating of the earth's surface by the sun, which in turn heats the lowest level of the atmosphere. In addition to simple thermal effects, atmospheric convection includes a large number of physical, chemical and biological processes at different scales. The study of atmospheric convection is usually performed by solving a large set of coupled non-linear equations which represent all these processes. These could be General Circulation Models (GCM) at the global scale or Cloud Resolving Models (CRM) at smaller scales. While they show realistic behaviour, their complexity, especially the large number of state variables in the models makes their results hard to interpret and can even obscure a more fundamental understanding of atmospheric processes.

In the context of atmospheric convection, moist convection (ie., convection in the presence of moisture) is one of the most important phenomenon in the tropics. Here, the release of latent heat due to phase changes in water is very important to the dynamics, while the micro-physical details of the nature, number and size of hydrometeors (water in liquid or solid form) have an important feedback on the convective scale dynamics. Recently several studies have focused on developing simplified models which ignore several processes at various scales but capture essential features of the real atmosphere - for some examples, see [4, 5, 6]. These studies considered moist convection with highly simplified cloud microphysics, moist convection with varying thermal boundary conditions and moist-convection without considering the dynamics of liquid water respectively. They found robust evidence of an up-down asymmetry (where hot, rising updrafts occupy a smaller fraction of the domain than cold, subsiding downdrafts) and scalings with different parameters for important measured quantities such as the heat-flux, the mass flux in clouds, the height of maximum cloud formation, etc. Further exploration of such simplified convective models with some basic processes of the atmosphere represented while omitting or greatly simplifying other processes has the potential to uncover which are the fundamental processes which set the dynamics of tropical moist convection and which do not greatly affect the behaviour of moist convection.

In this study, we focus on the simpler case of dry convection which occurs in the atmosphere when moisture is either absent or present in small enough quantities that condensation or freezing can be neglected. In other words, we consider convection of dry air or of moist air (i.e. with water vapor), but without phase change of water vapor into liquid or ice. For simplicity

we will derive the equations for dry air, but we note that water vapor could easily be accounted for by replacing temperature with virtual temperature [7]. Dry convection occurs in the region between the earth’s surface and the cloud-base, known as the sub-cloud layer. Dry convection is prevalent in the tropics over dry land and is particularly important in studies of the planetary boundary layer. Here, the constant cooling of the atmosphere by the emission of longwave radiation plays a non-negligible role in the dynamics.

To study this convective boundary layer, an idealisation that is most often made is to study the model fluid system with a fixed temperature at the lower boundary and (unlike Rayleigh-Bénard convection) a constant rate of diabatic cooling everywhere in the domain. An analysis of the stability of the system can be found in Chapter 3.6 of [7], while the results from more recent simulations are reported in [8].

Berlengiero et. al. in their study [9] (henceforth referred to as B2012) investigated the convective behaviour of a layer of fluid with a fixed heat-flux at the lower surface and a uniform bulk-cooling term to understand the basic features of atmospheric dry convection with a constant radiative cooling to space. They argued that in some scenarios, particularly over land, fixed-flux boundary conditions is a better representation of the heating of the atmosphere by the surface than fixed temperature. The system consists of a layer of a Boussinesq fluid with a fixed input heat-flux  $f_0$  at the lower surface, no vertical heat-flux at the upper boundary, a constant bulk-cooling  $-R$  and a set adiabatic temperature lapse rate  $\gamma$ . The heat input into the system and the cooling via the bulk-cooling term must be in global balance to ensure that a system at thermal equilibrium is achieved.

In B2012, the authors described the dynamics of two different 3D flows, one with a non-zero, finite temperature stratification and a second flow with no stratification. The results presented included the vertical temperature profile for both cases, the volume fraction of the domain occupied by up-draughts and the skewness of the vertical velocity. In particular, it was found that for both cases, less than half the volume was occupied by upward velocities, with concentrated intense hot plumes and large regions of subsiding flow. It was also found that the flow with  $\gamma = 0$  showed strong clustering of hot plumes due to the interaction between the rising plumes and the returning subsiding flow from the upper boundary.

This set-up has also been studied in [10], albeit for a adiabatic lapse-rate  $\gamma$  set to 0. The focus in their work was on the difference in the nature of the boundary layer and resulting net heat transfer when the heating was

distributed over a small height near the lower surface and not only the lower boundary.

In this study, we continue and expand the exploration of the internally cooled system for a wide-range of parameters, with the goal to derive scalings for important physical quantities, and identify different behaviors as a function of key adimensional parameters. We study and characterise how various important response parameters, particularly the temperature profiles, the up-down asymmetry and the total convective heat flux as well as the convective mass flux change with changing the various input parameters of the model. Further, we also add a discussion on the relevance to the scenario of dry atmospheric convection.

The article is laid out as follows. Section 2 discusses the basic equations of our model, a recap of the basic relations derived in B2012 and a description of the numerical methods. In Section 3 we derive some more analytical results, define appropriate length, velocity and temperature scales to derive the non-dimensional parameters characterising the system and end with a discussion on typical values for various parameters in the atmosphere. Section 4 presents the main results from our numerical simulations and we conclude with a discussion on the significance of the results as well as avenues for future work in Section 5.

## 2. Methodology: Equations and numerical simulations

### 2.1. Equations

As in B2012, we start with the incompressible Boussinesq fluid equations along with the heat equation with a bulk-cooling term. We thus write the density as the sum of a reference constant density  $\rho_{ref}$  and a perturbation from this reference density denoted by  $\rho'$  such that  $\rho = \rho_{ref} + \rho'$ , with corresponding pressure  $p = p_{ref}(z) + p'$  where  $p_{ref}(z)$  is in hydrostatic balance with  $\rho_{ref}$  so that  $dp_{ref}/dz = -\rho_{ref}g$ . The equations for the total fluid velocity vector  $\mathbf{u}$  with vertical component  $w$  and temperature fluctuations  $T'$  about a reference temperature  $T_{ref}$  are

$$\nabla \cdot \mathbf{u} = 0, \tag{1}$$

$$\partial_t \mathbf{u} + (\mathbf{u} \cdot \nabla) \mathbf{u} = -(1/\rho_{ref}) \nabla p' + \nu \nabla^2 \mathbf{u} - \beta T' \mathbf{g}, \tag{2}$$

$$\partial_t T' + \mathbf{u} \cdot \nabla T' + \gamma w = \kappa \nabla^2 T' - R, \tag{3}$$

where  $\nu$  is the kinematic viscosity,  $\beta$  is the thermal expansion coefficient,  $\mathbf{g} = -g\hat{z}$  is the acceleration due to gravity and  $\gamma = g/c_p$  is the lapse-rate of the mean stratification (or the dry adiabatic lapse-rate, see Appendix A).  $R$  ( $> 0$ ) is the bulk-cooling term applied to the fluid. As discussed by B2012, the term  $R$  breaks the up-down symmetry of the internally cooled system, leading to downward moving fluid ( $w < 0$ ) occupying more than half the domain.

Here we have assumed that the density perturbation  $\rho'$  is given by  $\rho'(T') = -\rho_{ref}\beta T'$ ,  $\rho_{ref}$  being the density of the fluid at temperature  $T_{ref}$ . For the Boussinesq approximation, it is only important that  $T'$  remains small enough that  $\rho(T)/\rho_{ref} \ll 1$  or equivalently,  $\beta T' \ll 1$ . For simplicity, we henceforth drop the primes and investigate equations (1) - (3) without the primes.

The velocity and the temperature fields are periodic in the horizontal directions. At the bottom ( $z = 0$ ) and top ( $z = L_z$ ) surfaces, they are given by

$$\mathbf{u}(z = 0) = \mathbf{u}(z = L_z) = 0 \quad (4)$$

and

$$\left. \frac{\partial T}{\partial z} \right|_{z=0} = -f_0, \quad \left. \frac{\partial T}{\partial z} \right|_{z=L_z} = -f_1. \quad (5)$$

It is noteworthy that this system is invariant under the transformation  $T \rightarrow T + \delta T$  where  $\delta T$  is some constant temperature since the heat equation as well as the boundary conditions contain only derivative terms of the temperature. In moist convection, this is no longer true as the partition of water into solid, liquid and gaseous phases strongly depends on the precise thermodynamic temperature.

In addition to the fluid equations, we recall from B2012 that the large-scale thermal balance for the system, which can easily be derived by taking the domain average of eqn. 3 in steady state, is given by

$$\kappa(f_0 - f_1) = RL_z. \quad (6)$$

As in B2012, we set  $f_0$  to be positive and  $f_1 = 0$ , leading to a balance between the radiative cooling in the domain and the net heat-flux from the boundaries. This also ensures that the average temperature of the domain remains stationary in time.

A steady-state solution for the equations with  $\mathbf{u} = 0$  everywhere leads to a temperature gradient

$$\frac{dT}{dz} = -f_0 \left( 1 - \frac{z}{L_z} \right) \quad (7)$$

with the corresponding temperature profile given by

$$T(z) = T_{bot} - zf_0 \left( 1 - \frac{z}{2L_z} \right), \quad (8)$$

where  $T_{bot}$  is the temperature at  $z = 0$ . The fluid is stably stratified where  $\partial_z T > -\gamma$ , which is given by  $z > L_z(1 - \gamma/f_0)$ . Thus we expect that when convection occurs, it occurs only up to a height  $z_0$  given by

$$z_0 = L_z(1 - \gamma/f_0). \quad (9)$$

## 2.2. Numerical Methods

In order to understand and investigate the behaviour of the above system, we solve the system of equations (1)-(5) numerically in a 2D domain box with fixed aspect ratio  $2\pi$  which is periodic in the horizontal direction. The various input parameters other than the extent of the domain are  $\gamma$ ,  $\kappa$ ,  $\nu$ , the product  $\beta g$  and  $f_0$ . We  $f_1$  is set to 0,  $\rho_{ref}$  to unity while  $R = \kappa f_0$  in accordance with the condition of thermal equilibrium (eqn. (6)). We also perform simulations for a horizontally periodic 3D domain with the same aspect ratio for a few selected parameters. The equations are solved with a python code employing the Dedalus spectral solver [11], using Fourier components in the periodic horizontal directions and Chebyshev polynomial decomposition for the vertical direction. The code was bench-marked against the results from B2012.

The outputs of the simulations are analysed to calculate various flow parameters only after the flow has become statistically stationary, wherein the average kinetic energy and the average temperature of the domain as well as the average temperature at the top and bottom surfaces of the domain fluctuate about a constant value. While we report only a few measurements from 3D runs, we have checked that all the below results are qualitatively true for 2D as well as 3D flows, unless otherwise mentioned.

### 3. Model Overview

#### 3.1. Exact Relations

In addition to the large-scale thermal balance and the steady-state temperature profile (eqns. (6) and (8)), we also derive the  $z$ -dependent thermal balance as is standard in the case of Rayleigh-Bénard convection and other model thermal fluid systems. Rewriting the advective term in flux-form ( $\nabla \cdot (\mathbf{u}T)$ ) and integrating the horizontal statistical average of eqn. (3) from the bottom to a height  $z$  gives

$$\langle wT \rangle_{A,t} - \kappa \langle \partial_z T \rangle_{A,t} = R(L_z - z), \quad (10)$$

where  $\langle \cdot \rangle_{A,t}$  indicates the statistical average taken at a fixed height  $z$  and we have used the fact that in the steady-state, the time-derivatives go to 0 while horizontal derivatives of the flux term average out to zero due to the periodic boundary conditions. This relation shows that the total vertical heat transfer by convection decays linearly as a function of height. Heat is removed uniformly at each height by the bulk radiative cooling term. In case of  $f_1$  not being set to 0, there would be an addition term  $\kappa f_1$  on the RHS which represents the outward heat-flux at the top of the domain.

For our system, we also calculate the global thermal dissipation  $\epsilon_T \equiv \kappa \langle |\nabla T|^2 \rangle$  given by (see Appendix B.1)

$$\begin{aligned} \kappa \langle |\nabla T|^2 \rangle &= \frac{\kappa}{L_z} T_{bot} f_0 - \gamma \langle wT \rangle - R \langle T \rangle \\ &= R \langle T_{bot} - T \rangle - \gamma \langle wT \rangle. \end{aligned} \quad (11)$$

where  $\langle \cdot \rangle$  indicates the statistical average taken over the whole domain and  $T_{bot}$  is the measured average temperature at  $z = 0$ . We can see that the RHS value still remains invariant under the transformation  $T \rightarrow T + \delta T$ . The strength of the thermal gradients in the fluid increases with the average departure of the domain temperature from  $T_{bot}$  and decreases when convective transfer of heat is efficient, that is  $\langle wT \rangle$  is large.

The viscous dissipation  $\epsilon \equiv (\nu/2) \sum_{i,j} (\partial u_i / \partial x_j + \partial u_j / \partial x_i)^2$  is given by (see Appendix B.2)

$$\frac{\nu}{2} \sum_{i,j} \left( \frac{\partial u_i}{\partial x_j} + \frac{\partial u_j}{\partial x_i} \right)^2 = \beta g \langle wT \rangle. \quad (12)$$

We can see that, similar to the Nusselt number in R-B convection, the response quantity  $\langle wT \rangle$  is of fundamental importance and it determines the convective heat transfer properties of the fluid system as well as the strength of the thermal and kinetic gradients. In the context of a convecting atmosphere, this value is the vertical buoyancy-flux, crucial in determining the thermodynamics of the atmosphere in shallow dry convection. In deep, moist convection too, the thermal flux in the sub-cloud layer is of crucial importance - for example it is approximately equal to the pressure-work done by the fluid and this is closely related to the production of irreversible entropy in the sub-cloud layer [12].

Analogous to the usual definition for R-B convection we define the Nusselt number Nus for the current system as

$$\text{Nus} = \frac{\langle wT \rangle}{\kappa T_0 / L_z} \quad (13)$$

where  $T_0$  is a temperature scale of the system to be defined later. The Nusselt number here compares the vertical heat-flux with the typical conductive heat flux. When the flow is conductive, we have no fluid motion and hence Nus = 0. In the presence of convection, Nus has a finite value which increases with the increase in the strength of convection.

### 3.2. Non-dimensional parameters

To quantify the system and non-dimensionalise the equations, we need appropriately defined temperature, velocity and length scales. Since the dynamics of the system is set by the bulk-cooling  $R$ , which has SI unit dimensions of Kelvin s<sup>-1</sup>, we can write the temperature scale  $T_0$  as

$$T_0 = R t_0 \quad (14)$$

where  $t_0$  is the appropriate time-scale, with length-scale  $L_z$  giving the velocity scale  $U_0 = L_z / t_0$ . As is standard for thermal flows, we write  $U_0$  as a convective velocity given by

$$U_0 = \sqrt{\beta g T_0 L_z}. \quad (15)$$

Combining the above equations gives finally

$$T_0 = (\beta g)^{-1/3} R^{2/3} L_z^{1/3}, \quad (16)$$

$$U_0 = (\beta g)^{1/3} R^{1/3} L_z^{2/3}, \quad (17)$$

$$t_0 = (\beta g)^{-1/3} R^{-1/3} L_z^{1/3}. \quad (18)$$

Using these scales, the equations are non-dimensionalised as

$$\widehat{\nabla} \cdot \widehat{\mathbf{u}} = 0, \quad (19)$$

$$\partial_{\widehat{t}} \widehat{\mathbf{u}} + (\widehat{\mathbf{u}} \cdot \widehat{\nabla}) \widehat{\mathbf{u}} = -\widehat{\nabla} \widehat{p} + \sqrt{\frac{\text{Pr}}{\text{Ra}}} \widehat{\nabla}^2 \widehat{\mathbf{u}} + \widehat{T} \widehat{z}, \quad (20)$$

$$\partial_{\widehat{t}} \widehat{T} + \widehat{\mathbf{u}} \cdot \widehat{\nabla} \widehat{T} + (\gamma/f_0) \sqrt{\text{Pr Ra}} \widehat{w} = \frac{1}{\sqrt{\text{Pr Ra}}} \widehat{\nabla}^2 \widehat{T} - 1, \quad (21)$$

where the hat ( $\widehat{\phantom{x}}$ ) indicates the non-dimensionalised variable or operator obtained by dividing by the appropriate dimensional scale. The non-dimensional parameters are the Rayleigh-Number  $\text{Ra}$ , the Prandtl number  $\text{Pr}$  and the ratio  $\gamma/f_0$  between the lapse-rate and heat-flux. The Rayleigh number is given by

$$\text{Ra} = (\beta g)^{2/3} \frac{R^{2/3} L_z^{10/3}}{\nu \kappa}. \quad (22)$$

This is equivalent to the form derived in B2012, albeit without appealing to a flux formulation. This equivalence is not surprising as the approach of B2012 (setting the time-scale of the fluid motion equal to the time-scale of radiative cooling) is identical to our approach in setting the temperature scale according to the rate of radiative cooling, which gives a non-dimensional rate of radiative cooling ( $RL_z/(U_0 T_0)$ ) of unity.  $\text{Ra}$  can also be re-written in terms of  $f_0$  using  $R^{2/3} L_z^{10/3} = (\kappa f_0)^{2/3} L_z^{8/3}$  from eqn. (6), which gives  $\text{Ra} \propto f_0^{2/3} / \kappa^{1/3}$ .

The Prandtl number is the ratio  $\nu/\kappa$  between the viscosity and the thermal conductivity. The ratio  $\gamma/f_0$  sets the height  $z_0$  above which the fluid is stably stratified (see Eqn. (9)). It can indeed be argued that the height  $z_0$  rather than  $L_z$  is the appropriate length scale to define the convective time and velocity-scales, which leads to a lapse-rate dependent Rayleigh number  $\text{Ra}_\gamma$  given by

$$\text{Ra}_\gamma = (\beta g)^{2/3} \frac{R^{2/3} z_0^{10/3}}{\nu \kappa} = \text{Ra} \left( 1 - \frac{\gamma}{f_0} \right)^{10/3}. \quad (23)$$

In this study, we solve the system of equations in arbitrarily chosen simulation units - however, all the results presented involve only non-dimensional quantities and it is the scaling with the non-dimensional parameters that we are interested in to characterise the system.

While several of our simulations have large differences of temperature between the lower and upper surface, thus invalidating the assumptions underlying the Boussinesq approximation, we note that this temperature difference is dictated by a combination of the temperature gradient at the lower boundary  $f_0$  and the lapse-rate  $\gamma$ . The principle of dynamic similarity for flows with the same  $\text{Ra}_\gamma$  can be used to construct an equivalent flow with  $f_0$  chosen to be an appropriately small value and also decreasing  $\kappa$  and  $\nu$  to retain the same  $\text{Ra}_\gamma$  ( $\propto f_0^{2/3} / \kappa^{1/3}$ ).

### 3.3. Some Orders of Magnitude

In the context of a typical scenario of dry convection in the tropics, convection occurs in a layer of atmosphere from the surface to cloud base level, which is 500 m to 3 km high, with the thermal heat flux (sensible heat flux) from the surface in the order of 10 – 100 W m<sup>-2</sup>, radiative cooling to space of 1 – 2 K day<sup>-1</sup> and dry air with a typical  $\beta \sim 1/300 \text{ K}^{-1}$ .

Sensible heat flux in W m<sup>-2</sup> can be converted to an equivalent thermal gradient by dividing by  $(\rho \kappa c_p)$  where  $\rho$  is the density and  $c_p$  is the heat capacity of air. When we consider an eddy-diffusivity like value of thermal conductivity  $\kappa \sim 10^{-2} \text{ m}^2 \text{ s}^{-1}$ , with  $\rho \sim 1 \text{ kg m}^{-3}$  and  $c_p \sim 10^3 \text{ J kg}^{-1} \text{ K}^{-1}$  we obtain  $f_0 \sim \mathcal{O}(1)$ . Considering the adiabatic lapse-rate to be the typical dry value of 0.01 K m<sup>-1</sup> and  $\beta g \sim 1/30 \text{ m s}^{-2} \text{ K}^{-1}$  gives  $\text{Ra}_\gamma$  to be at the least of order 10<sup>9</sup>. For the true molecular value of  $\nu$  and  $\kappa$ , the value of  $\text{Ra}_\gamma$  would be closer to 10<sup>15</sup>. It is important to note here that even for the lowest estimates of  $f_0$ ,  $\gamma$  is less than 1% of  $f_0$ <sup>i</sup>.

---

<sup>i</sup>If we consider real-world observations, it is well-known that ambient temperature measurements are recorded 2 metres above the land surface, which is typical a few Kelvin warmer than the air at the lowest level of the atmosphere on a sunny day. Thus, the temperature gradient at the boundary here is of the order of 1 Kelvin per metre, compared to the dry adiabatic lapse rate of 0.01 K m<sup>-1</sup>.

Parameter	Range
$Ra_\gamma$	(50, $10^6$ )
$\gamma/f_0$	(0, 0.75)
Pr	1

Table 1: The range of dimensionless parameters studied

$\gamma/f_0$	Critical $Ra_\gamma$
0	(130.162, 130.9497)
0.2	(86.966, 88.017)
0.4	(67.93, 69.3375)
0.75	(77.748, 78.412)

Table 2: The range of the critical  $Ra_\gamma$  for transition to convection found numerically for different values of  $\gamma/f_0$  in 2D. Flows with lower bound of  $Ra_\gamma$  were found to be stationary while flows with  $Ra_\gamma$  equal to the upper bound were found to be convective.

Given that the value of  $10 \text{ W m}^{-2}$  for the sensible heat-flux is a global annual average, there do exist scenarios where the sensible heat flux can be far smaller than this value. However, in these situations it is unrealistic to model the atmosphere to be locally in equilibrium with radiative cooling - instead the energy balance would be determined by large-scale, horizontal heat-fluxes or the cooling term would dominate the heat-equation. Studies of adjustment in such an out-of-equilibrium state is beyond the scope of the current study.

In using the current system as a model for atmospheric dry-convection, it is also important to assess the validity of the Boussinesq-approximation for dry convection. For a layer of atmosphere around 1 km thick, temperature differences  $\Delta T$  between the bottom and the top of this layer are of the order of  $\sim 10 \text{ K}$ , as the atmosphere remains close to a dry adiabatic profile. This translates to  $\beta\Delta T \approx 3 \times 10^{-2}$ . Thus, we see that the Boussinesq approximation remains an excellent approximation in the simulation of dry convection. In the presence of moisture and the ensuing deep, moist convection that penetrates up to the top of the troposphere ( $\sim 15 \text{ km}$ ), the Boussinesq approximation breaks down and the vertical variation in density is significant.

From the above discussion it is clear that the current model under investigation is valid for shallow, sub-cloud dry convection where it can be assumed that the convection and sensible heat-flux is locally in equilibrium with the cooling of the atmosphere through outgoing long-wave radiation to space. In Table 1, we show the range of dimensionless parameters simulated in the current study.

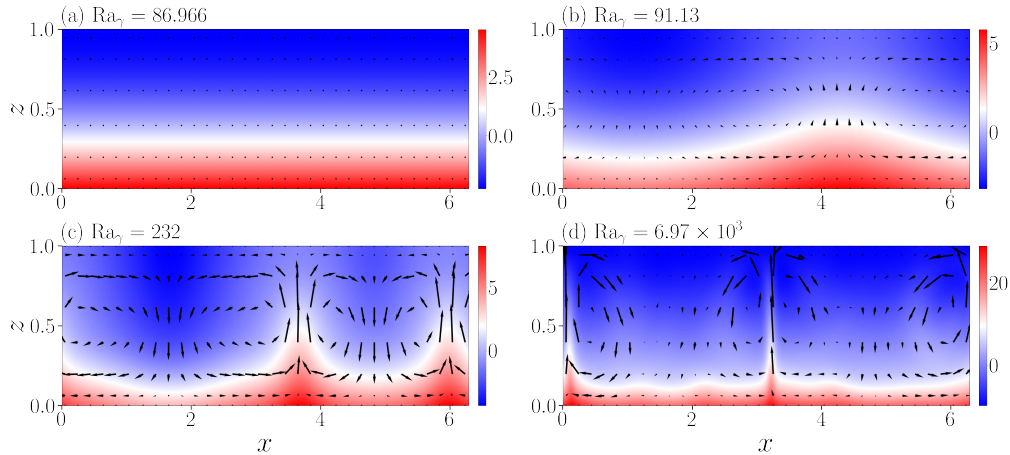


Figure 1: Instantaneous snapshots of the temperature field  $T$  in the stationary regime for flows with different  $Ra_\gamma$  as indicated in the figure and  $\gamma/f_0 = 0.2$ . The temperature fields are divided by the respective temperature scale  $T_0$  defined in Eqn. (16) and scaled such their domain average is 0. Panel (a) shows a stable flow while panels (b), (c) and (d) show convective flows. The arrows represent velocity vectors with the arrow length in plot units equal to velocity magnitude divided by  $U_0$ ,  $U_0$ ,  $2U_0$  and  $5U_0$  respectively where  $U_0$  is the velocity scale defined in Eqn. (17).

## 4. Results

### 4.1. Transition to convection

With  $\gamma = 0$ , it is found that for very small values of  $f_0$  (or equivalently, small values of  $R$ ), the flow remains motionless ( $\mathbf{u} = \mathbf{0}$ ) and assumes a temperature profile given by Eqn. (8). When  $f_0$  is increased beyond a critical value, the flow becomes convective with convective rolls that extend up to height  $L_z$  since  $z_0 = L_z$  when  $\gamma = 0$ . For finite values of  $\gamma$ , the flow remains stable for larger values of  $f_0$  than for the  $\gamma = 0$  case. On increasing  $f_0$  beyond the critical value, the flow becomes convective where the convective rolls extend up to height  $z_0$ . For the case of  $\gamma = f_0$ , the flow is always stable as in this case no heat-transfer occurs from the lower surface to the fluid. We find numerically that the critical  $Ra_\gamma$  for the triggering of convection depends weakly on the ratio  $\gamma/f_0$ . The numerically estimated values using 2D simulations are given in Table 2. The goal of the current study is to characterise the behaviour of the fully convective regime rather than a detailed study of the fluid instability. We note however that the estimation of the critical  $Ra_\gamma$  for different values of  $\gamma$  should be analytically

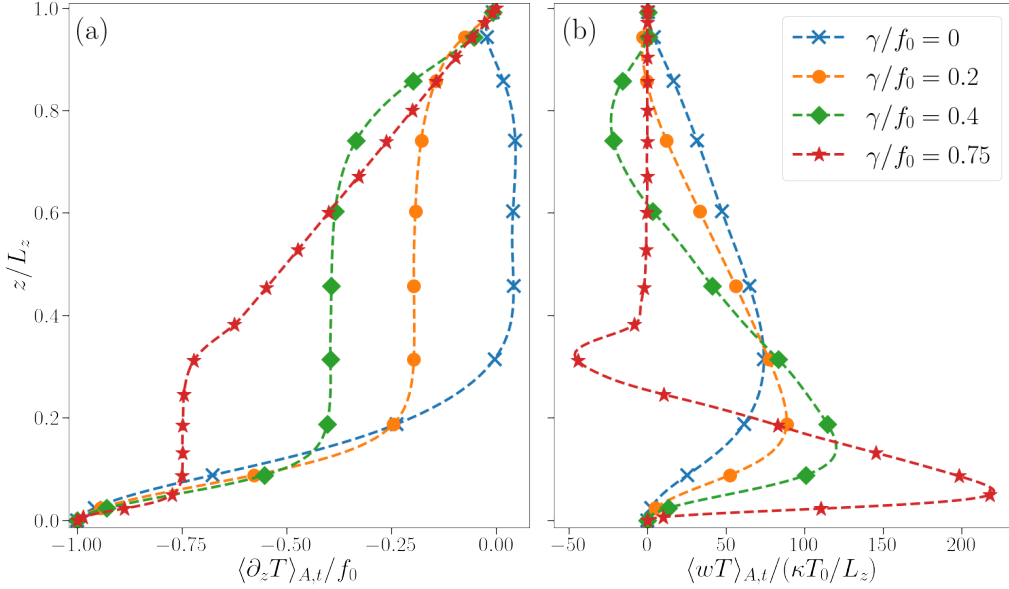


Figure 2: (a) Average vertical profiles of  $\partial_z T$  divided by  $f_0$ . (b) Average vertical profiles of  $wT$  divided by  $\kappa T_0 / L_z$ . Both panels share the same legend, with the flows having  $\text{Ra}_\gamma \sim 10^4$  and the averages are statistical, height-wise averages for each flow.

tractable through the analysis into normal modes of a small perturbation on the steady-state solution as is usually done for classical Rayleigh-Bénard convection (for example see [13]) and other instabilities.

Figure 1 shows instantaneous snapshots of the linearly scaled, non dimensionalised temperature field for 2D flows with  $\gamma/f_0 = 0.2$ . When the flow is stable (see panel (a)), the fluid is held motionless by viscosity and thermal dissipation and the temperature field is perfectly homogeneous in the horizontal direction. When  $f_0$  is increased slightly, as in panel (b), the flow shows a pattern of large, space-filling convective rolls. Larger values of  $f_0$  shown in the lower panels show intense and clearly defined rising convective plumes, where the hot, rising plumes have a large positive height-wise temperature anomaly, while the gently subsiding regions outside these plumes have a smaller negative height-wise temperature anomaly. In panel (d), the hot plume is the narrowest with the highest velocities (seen by length of the arrows) strongly concentrated in the rising plumes. The reader should note that the arrows representing the velocity fields are scaled by a different value in each panel only to ensure clarity in the figure - arrow lengths must not be

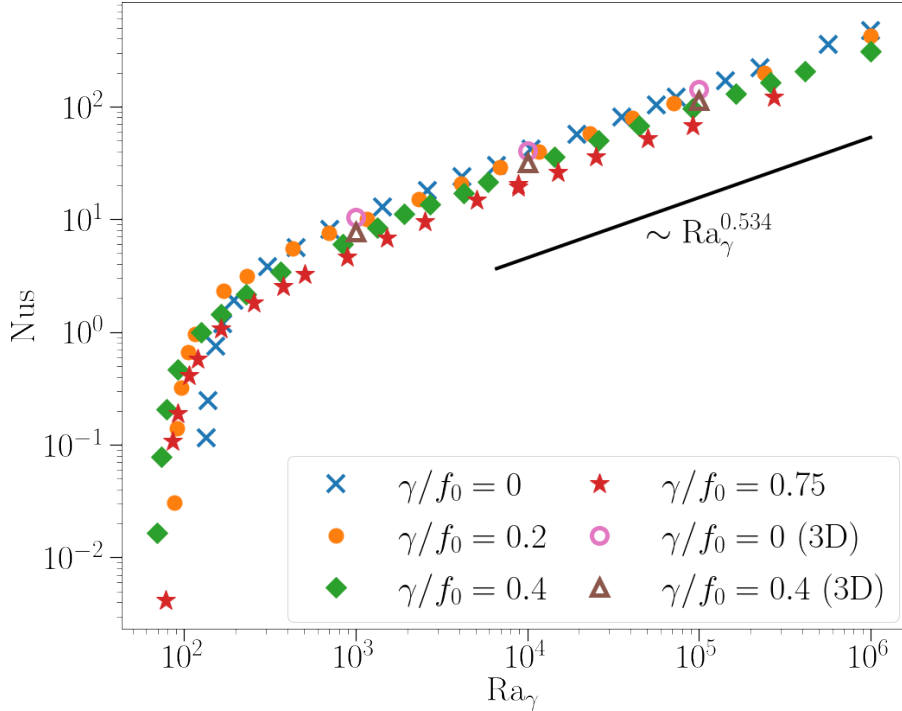


Figure 3: Nusselt number of the flow as a function of  $Ra_\gamma$  for 4 different values of  $\gamma/f_0$  in 2D and 2 different values in 3D.

used to compare the velocity between different panels.

#### 4.2. Flow structures and Profiles

In the convective regime, intense hot plumes arise from the lower surface along with broad regions of cold subsidence. There exists a small diffusive boundary layer near the lower surface underneath the intense hot plumes. Here, the vertical gradient of the temperature field ( $\partial_z T$ ) quickly goes from  $-f_0$  to  $-\gamma$  as seen in Figure 2(a). Above this layer lies a convective bulk region where the effective mixing of the fluid ensures  $\partial_z T \approx -\gamma$  up to a height of approximately  $z_0$ . For small  $\gamma$ , this corresponds to the top of the domain and thus there is no conducting region close to the upper boundary. Above  $z_0$ ,  $\partial_z T$  goes to 0 at  $z = L_z$  in a linear fashion, which corresponds to the stable layer above the convective layer.

Panel (b) of Figure 2 shows the time-averaged convective flux divided by the product of a diffusive velocity scale  $\kappa/L_z$  and the temperature scale

$T_0$  - that is the height-wise Nusselt number. The convective flux attains a maxima at  $z$  roughly corresponding to the end of the lower thermal boundary layer. Above this layer and up to  $z = z_0$ , ie., in the convective region where  $\partial_z T$  remains nearly constant, the flux decreases linearly consistent with eqn. (10).

For larger values of  $\gamma$ , there exists a small layer of fluid close to  $z \gtrsim z_0$  where the flux is negative - this can be explained by the formation of cold patches of fluid above the rising thermal plumes. The fast rising parcels of fluid are cooled rapidly due to the lapse-rate term, leading to a region where the fluid is colder than the horizontal average while the fluid is still rising ( $w > 0$ ), leading to a negative flux. Above this, the fluid is no longer convecting, leading to a flux close to 0. Thus, in the presence of a large lapse-rate, the domain-averaged convective heat-flux (Nus) is partially decreased by the strong cooling of fast-rising parcels of fluid.

#### 4.3. The Nusselt Number

The convective heat-flux characterises the behaviour of the flow to a large degree, as it determines the strength of the velocity and temperature gradients and also plays an import role in understanding the behaviour of the fluid in the viscous boundary layers. The non dimensionalised heat-flux, the Nusselt number (defined in Eqn. (13)) is thus particularly important in understanding the convective behaviour of the system.

The Nusselt number is identically 0 for conductive flows as the fluid is not in motion. In the convective regime, Nus increases with increasing  $Ra_\gamma$  as we see in figure 3, which shows the scaling of the Nusselt number for changing  $Ra_\gamma$  and for various values of  $\gamma/f_0$ . For flows with identical  $Ra_\gamma$ , Nus is the largest for the cases with  $\gamma = 0$ . This is due to the fact that for flows without an imposed lapse rate, the convection is penetrative ( $z_0 = L_z$ ) and the hot plumes reach the top of the domain. In the case of flows with a finite lapse rate, the region of the flow above  $z_0$  contributes negatively to the total convective heat flux of the system, as already discussed in the previous section and seen in Figure 2(b). We note that this contribution is quite small, given that the values are nearly identical for  $\gamma/f_0$  ranging from 0 to 0.75. This also indicates that  $Ra_\gamma$  is a well-chosen parameter to characterise the large-scale behaviour of this model system.

The magnitude and scaling of the Nusselt number as a function of  $Ra_\gamma$  for 3D flows is identical to the 2D flows. This indicates that in making estimates

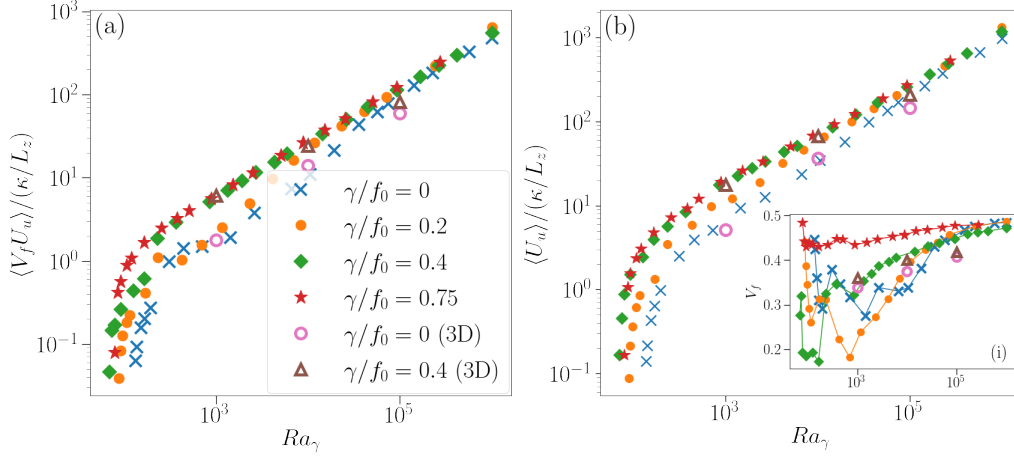


Figure 4: (a) Domain-averaged convective mass flux plotted against  $Ra_\gamma$  for 4 different values of  $\gamma/f_0$  in 2D and 2 values of  $\gamma/f_0$  in 3D. The mass flux is non-dimensionalised by dividing it by the diffusive velocity scale  $\kappa/L_z$ . (b) Average velocity  $U_u$  in regions of the flow where  $w > 0$  divided by the diffusive velocity scale as a function of  $Ra_\gamma$  for the same parameters as panel (a). Inset (i) shows the volume fraction  $V_f$  of the domain occupied by updrafts ( $w > 0$ ).

of dry convective heat-fluxes with given boundary conditions, it is sufficient to simulate a 2D domain.

#### 4.4. Mass-flux, Updraft Velocities and Up-down Asymmetry

Along with the convective heat-flux, the convective mass-flux also remains an important parameter to be estimated in thermal flows, particularly in the dry atmosphere. The mass flux at a given height is calculated as the product of the volume fraction  $V_f$  of the domain which is rising ( $w > 0$ ) and the average vertical velocity  $U_u$  within these rising regions. The total convective mass flux is the vertical average of the mass-flux at each height written as  $\langle V_f U_u \rangle$ .

The variation of the convective mass-flux with  $Ra_\gamma$  is shown in panel (a) of figure 4. We see that the mass flux close to the transition to convection shows large variation in magnitude depending on the value of  $\gamma/f_0$ , with the mass flux being greater for the flows with greater  $\gamma/f_0$ . This is similar to the behaviour of the Nusselt number. For large enough  $Ra_\gamma$ , all values of mass-flux converge to a single line on the log-log plot, which corresponds to an exponential dependence on  $Ra_\gamma$ . The updraft velocities  $U_u$  and the volume

fraction  $V_f$  are shown in panel (b) and inset (i) respectively. For larger values of  $\text{Ra}_\gamma$  the values of  $U_u$  also converge to a single exponent independent of  $\gamma/f_0$  while  $V_f$  converges to a single value  $\sim 0.48$ .

The variation of  $V_f$  with increasing  $\text{Ra}_\gamma$  can be explained from the behavior seen in Figure 1 - when the flow is convective and laminar (as is the case for small  $\text{Ra}_\gamma$  close to the critical value for transition) the only upward moving regions occur in the vicinity of the rising plume, and the entire domain is filled by a single, large convective roll. The rest of the domain is uniformly, weakly subsiding. This behaviour can be observed for example on closer examination of panel (b) in Figure 1, where a part of domain extending from approximately  $x = 3$  to  $x = 5.5$  is a clearly delineated upward rising region and the rest of the domain is subsiding with a much smaller velocity to compensate for the rising mass in the rising plume. For larger  $\text{Ra}_\gamma$  flows which are more turbulent and have greater kinetic energy, the flow contains multiple plumes and convective rolls with rapid point-wise temporal fluctuations in velocity. For example, in panel (d) of the same figure, while the region between  $x \approx 1$  to  $x \approx 2.5$  is subsiding on average, some grid points individually have  $w > 0$  within this region. For the largest values of  $\text{Ra}_\gamma$ , the flows are highly turbulent and energetic, leading to a  $V_f$  value close to half.

The asymmetry between up and down that results from the  $-R$  term is important only in the convective region of the flow. The stable upper layer in flows with non-zero  $\gamma$  are locally in conductive equilibrium and fluid motion here is only due to the transport of mass and momentum from the convective region. These regions do not show an up-down asymmetry. Thus, regions with a thicker stable layer (larger  $\gamma/f_0$ ) are overall more symmetric and the domain average  $V_f$  is closer to half, independent of  $\text{Ra}_\gamma$ .

The mass flux and the updraft velocity scales nearly identically in 2D as well as 3D, though in the 3D case  $V_f$  converges to a value close to half for much larger  $\text{Ra}_\gamma$  (if we assume that the scaling seen in Figure 3(i) holds for larger  $\text{Ra}_\gamma$ ). Simulations for 3D flows with  $\text{Ra}_\gamma > 10^5$  were not performed due to the requirement of large computing resources and are beyond the scope of this study.

While the volume fraction  $V_f$  gives an insight into the degree of asymmetry in the flow, it does not capture the relative magnitude of the velocity of rising and subsiding regions, thus does not fully quantify the asymmetry. Another measure often used (including in B2012) is the skewness measure of the vertical velocity field. The skewness  $S$  is defined as

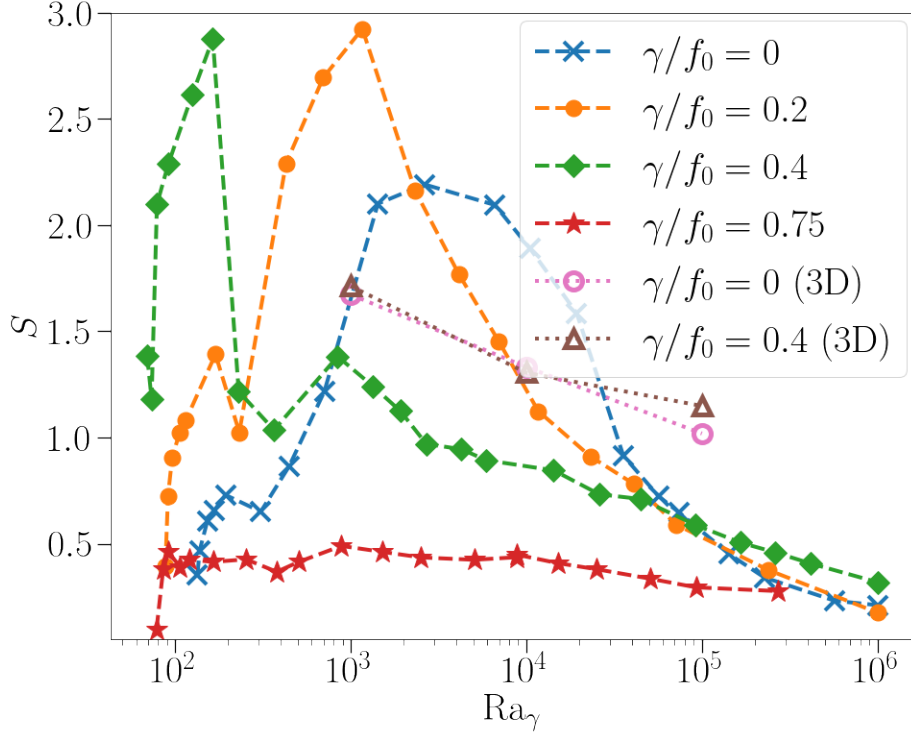


Figure 5: Skewness  $S$  of the vertical velocity for flows with varying  $\gamma/f_0$  as a function of  $Ra_\gamma$  for 2D and 3D simulations.

$$S = \frac{\langle w^3 \rangle}{(\langle w^2 \rangle)^{3/2}}, \quad (24)$$

where we have used the fact that  $\langle w \rangle = 0$ . A positive skew implies a left-peaked distribution, where the tail on the positive end is thicker while the median  $w$  is negative. Figure 5 shows  $S$  as a function of  $Ra_\gamma$  for various values of  $\gamma/f_0$ .  $S$  follows a trend which is close to the inverse of  $V_f$  (see figure 4(i)), where the value of  $S$  peaks when the value of  $V_f$  is at a minima. Similar to  $V_f$ , the skewness also converges to a value which is between 0 and 0.5 for large  $Ra_\gamma$ , consistent with the aforementioned small-degree of asymmetry.

It is the  $-R$  term that breaks the up-down asymmetry - however we see that for greater  $R$ , the flow becomes less asymmetric. Whereas the flows with

the largest degree of asymmetry have  $R$  just large enough to overcome the stabilisation by viscous forces. We note here that the key factor determining the asymmetry is the relative importance of the bulk-cooling term. Considering the non-dimensionalised heat-equation, eqn. (21), the LHS value is large when the typical magnitude of fluctuations in  $\hat{T}$  and  $\hat{\mathbf{u}}$  are large. This is the case when  $Ra$  is large. For cases of smaller and intermediate values of  $Ra$ , the magnitude of fluctuations in  $\hat{T}$  and  $\hat{\mathbf{u}}$  are small, so the cooling term is relatively more important in the dynamics.

## 5. Discussion and Conclusions

We have presented results from 2D as well as 3D simulations of an uniformly cooled thermal fluid system in the presence of gravity and a lapse rate with a uniform heat flux at the lower surface and an adiabatic (no heat flux) boundary condition for the top surface. The fluid is assumed to be incompressible and we work in the regime of the Boussinesq approximation, which is a fair approximation for the sub-cloud layer of the earth's atmosphere, where the atmosphere is either dry or moist-unsaturated. The constant, bulk cooling term is set such that it balances the incoming heat flux at the lower surface, leading to a situation where there is balance between a constant cooling of the domain and a heating from below, which is analogous to the atmosphere which is heated by the earth surface and constantly loses heat to space through longwave radiation. The current work is a direct extension of previous work by Berlingiero et. al. reported in B2012.

The equations are non-dimensionalised using a temperature and velocity scale based on the magnitude of the diabatic cooling term. For the length-scale, we choose the height up to which the domain is unstable to dry convection  $z_0$ , where  $z_0$  depends on the ratio between the lapse-rate  $\gamma$  and the uniform flux at the lower surface  $f_0$ . This leads to the lapse-rate dependent Rayleigh number denoted  $Ra_\gamma$  which characterises the system well.

We show that when  $Ra_\gamma$  is small, the dissipation of heat and momentum is sufficient to have a motionless steady-state solution for the fluid with all the heat transfer occurring through thermal conductivity alone. Beyond a critical value, the fluid no longer remains motionless and is unstable to small perturbations which induce a convective motion in the system. We have further shown that in this convective regime, the scaling of important measured quantities such as the Nusselt number, the non-dimensionalised mass-flux and average velocity in updrafts with  $Ra_\gamma$  converge to a single

exponent, with some dependence of the magnitude on the dimensionless ratio  $\gamma/f_0$ . The bulk cooling term also introduces an up-down asymmetry in the fluid - this asymmetry is particularly marked when the flow is only weakly convective, ie.  $Ra_\gamma$  is only slightly larger than the critical value. For strongly convective flows, the degree of the asymmetry as measured by the volume of the domain occupied by updrafts (regions where  $w > 0$ ) and the skewness of the vertical velocity decreases, where nearly half the domain is made up of updrafts and the skewness goes close to 0. While the 3D flows are identical to the 2D flows in the scaling of heat and mass transfers with  $Ra_\gamma$ , they retain a large degree of up-down asymmetry even at  $Ra_\gamma \sim 10^5$ .

In this study, we have added to the existing body of literature on various models of thermal convective systems which help us understand atmospheric convection under different conditions. While the system has been introduced elsewhere, this is to the best of our knowledge the first study that systematically varies the parameters for a fixed-flux, internally cooled convective system, a system with particular relevance to the sub-cloud atmospheric boundary layer. Our main aim here has been to demonstrate the simple scaling of the system with respect to various input parameters and provoke future studies which explore higher Rayleigh numbers as well as mixed boundary conditions and non-uniform radiative cooling.

Idealised models of convection, including those with moisture and water phase changes serve to provide a tool to study the complex atmospheric system in a simplified setting where it is far easier to delineate the dynamic effects and feedbacks due to individual processes. In the future, we plan to study idealised models which include moist dynamics as well as global-scale idealised models which include the effects of rotation.

## Acknowledgments

This project has received funding from the European Union’s Horizon 2020 research and innovation programme under the Marie Skłodowska-Curie grant agreement No. 101034413. CM gratefully acknowledges funding from the European Research Council (ERC) under the European Union’s Horizon 2020 research and innovation program (Project CLUSTER, Grant Agreement No. 805041).

## Conflict of Interests and Data Availability

The authors declare no conflicts of interest. Datasets and the code used to generate the data are available from the authors upon reasonable request.

## Appendix A. The heat-equation

We start with the first law of thermodynamics in enthalpy form given by

$$c_p \frac{DT}{Dt} - \frac{1}{\rho} \frac{Dp}{Dt} = \dot{Q} \quad (\text{A.1})$$

where  $m$  is the mass of the fluid parcel,  $c_p$  is the specific heat-capacity at constant pressure and  $\dot{Q}$  is the rate of diabatic heating or cooling per unit mass. We make the assumption ( $D_t p \approx w \partial_z p_{ref} \approx -\rho_{ref} g w$ ), which is the condition of hydrostatic balance. This also assumes that a given parcel always has the same pressure as its environment, which is a common assumption made in parcel theory. This gives,

$$\partial_t T + \mathbf{u} \cdot \nabla T + (g/c_p)w = \dot{Q}/c_p, \quad (\text{A.2})$$

where the RHS includes thermal dissipation as well as diabatic cooling, which is given by  $-R$  in this study.  $g/c_p \equiv \gamma$  is the well known dry adiabatic lapse-rate.

## Appendix B. Thermal and Viscous dissipation

### Appendix B.1. Thermal Dissipation

The thermal dissipation is defined as

$$\epsilon_T \equiv \kappa \langle (\partial_i T(\mathbf{x}, t))^2 \rangle_V. \quad (\text{B.1})$$

Following [?]’s analysis for Rayleigh-Bénard convection, we multiply equation (3) by temperature  $T$  and average the product over the entire domain and time to give

$$\begin{aligned} \frac{1}{2} \frac{d\langle T^2 \rangle}{dt} + \frac{1}{2} \langle \mathbf{u} \cdot \nabla (T^2) \rangle + \gamma \langle wT \rangle + \langle RT \rangle \\ = \kappa \langle T \nabla^2 T \rangle = \kappa \langle \nabla \cdot (T \nabla T) \rangle - \kappa \langle |\nabla T|^2 \rangle, \end{aligned} \quad (\text{B.2})$$

Since we working in the stationary regime, ( $\partial_t \langle \cdot \rangle = 0$ ). Further, using the incompressibility condition (eq. (1)) and the fluid rigid boundary condition ((4)), we get

$$\langle \mathbf{u} \cdot \nabla (T^2) \rangle_V = \langle \nabla \cdot (\mathbf{u} T^2) \rangle_V = 0. \quad (\text{B.3})$$

Then, equation (B.2) becomes

$$\kappa \langle |\nabla T|^2 \rangle = \kappa \langle \nabla \cdot (T \nabla T) \rangle - \gamma \langle wT \rangle - R \langle T \rangle, \quad (\text{B.4})$$

or

$$\epsilon_T = \kappa \langle \nabla \cdot (T \nabla T) \rangle - \gamma \langle wT \rangle - R \langle T \rangle. \quad (\text{B.5})$$

Using the Gauss theorem, the first term of  $\epsilon_T$  can be written in terms of a surface integral as

$$\kappa \langle \nabla \cdot (T \nabla T) \rangle = \frac{\kappa}{L_z} \left[ \langle T \partial_z T \rangle_{z=L_z} - \langle T \partial_z T \rangle_{z=0} \right]. \quad (\text{B.6})$$

Setting  $\partial_z T|_{z=0} = -f_0$  and  $\partial_z T|_{z=L_z} = -f_1 = 0$  gives the expression in eqn. (11)

$$\kappa \langle |\nabla T|^2 \rangle = \frac{\kappa}{L_z} (T_0 f_0) - \gamma \langle wT \rangle - R \langle T \rangle. \quad (\text{B.7})$$

### *Appendix B.2. Viscous Dissipation*

Taking the dot product of eq. (2) with  $\mathbf{u}$  and taking the statistical average over the whole volume as above, we get

$$\begin{aligned} \frac{1}{2} \frac{d}{dt} \langle (\mathbf{u} \cdot \mathbf{u}) \rangle + \frac{1}{2} \langle \mathbf{u} \cdot \nabla (\mathbf{u} \cdot \mathbf{u}) \rangle \\ = - \langle \mathbf{u} \cdot \nabla p \rangle + \nu \langle \mathbf{u} \cdot \nabla^2 \mathbf{u} \rangle + \beta g \langle wT \rangle. \end{aligned} \quad (\text{B.8})$$

In the stationary state, the terms of the form  $d_t \langle \cdot \rangle$  vanish. Using the incompressibility condition and the rigid boundary condition, we have

$$\langle \mathbf{u} \cdot \nabla (\mathbf{u} \cdot \mathbf{u}) \rangle_V = \langle \nabla \cdot [\mathbf{u} (\mathbf{u} \cdot \mathbf{u})] \rangle_V = 0 \quad (\text{B.9})$$

$$\langle \mathbf{u} \cdot \nabla p \rangle_V = \langle \nabla \cdot (\mathbf{u} p) \rangle_V = 0 \quad (\text{B.10})$$

$$\begin{aligned}
\langle \mathbf{u} \cdot \nabla^2 \mathbf{u} \rangle_V &= \frac{1}{2} \langle \nabla \cdot \nabla (\mathbf{u} \cdot \mathbf{u}) \rangle_V - \sum_{i,j} \left\langle \left( \frac{\partial u_j}{\partial x_i} \right)^2 \right\rangle_V \\
&= - \sum_{i,j} \left\langle \left( \frac{\partial u_j}{\partial x_i} \right)^2 \right\rangle_V \\
&= - \frac{1}{2} \sum_{i,j} \left\langle \left( \frac{\partial u_i}{\partial x_j} + \frac{\partial u_j}{\partial x_i} \right)^2 \right\rangle_V.
\end{aligned} \tag{B.11}$$

So, equation (B.8) becomes

$$\frac{\nu}{2} \sum_{i,j} \left\langle \left( \frac{\partial u_i}{\partial x_j} + \frac{\partial u_j}{\partial x_i} \right)^2 \right\rangle = \beta g \langle wT \rangle, \tag{B.12}$$

or

$$\epsilon \equiv \frac{\nu}{2} \sum_{i,j} \left\langle \left( \frac{\partial u_i}{\partial x_j} + \frac{\partial u_j}{\partial x_i} \right)^2 \right\rangle = \beta g \langle wT \rangle. \tag{B.13}$$

## References

- [1] J. Thomson, et al., On a changing tessellated structure in certain liquids, Proc. Phil. Soc. Glasgow 13 (1882) 464–468.
- [2] H. Bénard, Les tourbillons cellulaires dans une nappe liquide.-méthodes optiques d’observation et d’enregistrement, Journal de Physique Théorique et Appliquée 10 (1901) 254–266.
- [3] L. Rayleigh, Lix. on convection currents in a horizontal layer of fluid, when the higher temperature is on the under side, The London, Edinburgh, and Dublin Philosophical Magazine and Journal of Science 32 (1916) 529–546.
- [4] G. Hernandez-Duenas, A. J. Majda, L. M. Smith, S. N. Stechmann, Minimal models for precipitating turbulent convection, Journal of Fluid Mechanics 717 (2013) 576–611.
- [5] T. Weidauer, J. Schumacher, Moist turbulent rayleigh-bénard convection with neumann and dirichlet boundary conditions, Physics of Fluids 24 (2012) 076604.

- [6] G. K. Vallis, D. J. Parker, S. M. Tobias, A simple system for moist convection: the rainy–bénard model, *Journal of Fluid Mechanics* 862 (2019) 162–199.
- [7] K. A. Emanuel, *Atmospheric convection*, Oxford University Press, USA, 1994.
- [8] T. Hartlep, F. H. Busse, Convection in an internally cooled fluid layer heated from below, *Geophysical & Astrophysical Fluid Dynamics* 112 (2018) 20–35.
- [9] M. Berlingiero, K. Emanuel, J. Von Hardenberg, A. Provenzale, E. Spiegel, Internally cooled convection: a fillip for philip, *Communications in Nonlinear Science and Numerical Simulation* 17 (2012) 1998–2007.
- [10] S. Lepot, S. Aumaître, B. Gallet, Radiative heating achieves the ultimate regime of thermal convection, *Proceedings of the National Academy of Sciences* 115 (2018) 8937–8941.
- [11] K. J. Burns, G. M. Vasil, J. S. Oishi, D. Lecoanet, B. P. Brown, Dedalus: A flexible framework for numerical simulations with spectral methods, *Physical Review Research* 2 (2020) 023068.
- [12] K. A. Emanuel, M. Bister, Moist convective velocity and buoyancy scales, *Journal of the atmospheric sciences* 53 (1996) 3276–3285.
- [13] S. Chandrasekhar, *Hydrodynamic and hydromagnetic stability*, Courier Corporation, 2013.